

# Tunable and switchable dual-wavelength Tm-doped mode-locked fiber laser by nonlinear polarization evolution

Zhiyu Yan,<sup>1,2</sup> Xiaohui Li,<sup>1</sup> Yulong Tang,<sup>1</sup> Perry Ping Shum,<sup>1</sup> Xia Yu,<sup>2,4</sup> Ying Zhang,<sup>2</sup> and Qi Jie Wang<sup>1,3,5</sup>

<sup>1</sup>OPTIMUS, Photonics Center of Excellence, School of Electrical and Electronic Engineering, Nanyang Technological University, 50 Nanyang Ave., 639798, Singapore

<sup>2</sup>Precision Measurements Group, Singapore Institute of Manufacturing Technology, 71 Nanyang Drive, 638075, Singapore

<sup>3</sup>COFT, Centre for Optical Fiber Technology, Nanyang Technological University, 637371, Singapore

<sup>4</sup>[xyu@simtech.a-star.edu.sg](mailto:xyu@simtech.a-star.edu.sg)

<sup>5</sup>[qjwang@ntu.edu.sg](mailto:qjwang@ntu.edu.sg)

**Abstract:** We propose and demonstrate a tunable and switchable dual-wavelength ultra-fast Tm-doped fiber laser. The tunability is based on nonlinear polarization evolution (NPE) technique in a passively mode-locked laser cavity. The NPE effect induces wavelength-dependent loss in the cavity to effectively alleviate mode competition and enables the multiwavelength mode locking. The laser exhibits tunable dual-wavelength mode locking over a wide range from 1852 to 1886 nm. The system has compact structure and both the wavelength tuning and switching capabilities can be realized by controlling the polarization in the fiber ring cavity.

©2015 Optical Society of America

**OCIS codes:** (140.3510) Lasers, fiber; (140.3600) Lasers, tunable; (140.4050) Mode-locked lasers.

---

## References and links

1. Z. W. Xu and Z. X. Zhang, "All-normal-dispersion multi-wavelength dissipative soliton Yb-doped fiber laser," *Laser Phys. Lett.* **10**(8), 085105 (2013).
2. X. Li, Y. Wang, Y. Wang, X. Hu, W. Zhao, X. Liu, J. Yu, C. Gao, W. Zhang, Z. Yang, C. Li, and D. Shen, "Wavelength-switchable and wavelength-tunable all-normal-dispersion mode-locked Yb-doped fiber laser based on single-walled carbon nanotube wall paper absorber," *IEEE Photon. J.* **4**(1), 234–241 (2012).
3. H. Zhang, D. Y. Tang, X. Wu, and L. M. Zhao, "Multi-wavelength dissipative soliton operation of an erbium-doped fiber laser," *Opt. Express* **17**(15), 12692–12697 (2009).
4. X. Zhao, Z. Zheng, L. Liu, Y. Liu, Y. Jiang, X. Yang, and J. Zhu, "Switchable, dual-wavelength passively mode-locked ultrafast fiber laser based on a single-wall carbon nanotube modelocker and intracavity loss tuning," *Opt. Express* **19**(2), 1168–1173 (2011).
5. A. Y. Chamorovskiy, A. V. Marakulin, A. S. Kurkov, and O. G. Okhotnikov, "Tunable Ho-doped soliton fiber laser mode-locked by carbon nanotube saturable absorber," *Laser Phys. Lett.* **9**(8), 602–606 (2012).
6. S. Wang, P. Lu, S. Zhao, D. Liu, W. Yang, and J. Zhang, "2- $\mu$ m switchable dual-wavelength fiber laser with cascaded filter structure based on dual-channel Mach-Zehnder interferometer and spatial mode beating effect," *Appl. Phys. B* **117**(2), 563–569 (2014), doi:10.1007/s00340-014-5868-0.
7. X. Feng, H. Y. Tam, and P. K. A. Wai, "Stable and uniform multiwavelength erbium-doped fiber laser using nonlinear polarization rotation," *Opt. Express* **14**(18), 8205–8210 (2006).
8. Z. Luo, A. Luo, W. Xu, H. Yin, J. Liu, Q. Ye, and Z. Fang, "Tunable multiwavelength passively mode-locked fiber ring laser using intracavity birefringence-induced comb filter," *IEEE Photon. J.* **2**(4), 571–577 (2010).
9. S. Pan and C. Lou, "Stable multiwavelength dispersion-tuned actively mode-locked erbium-doped fiber ring laser using nonlinear polarization rotation," *IEEE Photon. Technol. Lett.* **18**(13), 1451–1453 (2006).
10. T. V. A. Tran, K. Lee, S. B. Lee, and Y. G. Han, "Switchable multiwavelength erbium doped fiber laser based on a nonlinear optical loop mirror incorporating multiple fiber Bragg gratings," *Opt. Express* **16**(3), 1460–1465 (2008).
11. W. Peng, F. Yan, Q. Li, S. Liu, T. Feng, and S. Tan, "A 1.97  $\mu$ m multiwavelength thulium-doped silica fiber laser based on a nonlinear amplifier loop mirror," *Laser Phys. Lett.* **10**(11), 115102 (2013).

12. X. Li, X. Liu, D. Mao, X. Hu, and H. Lu, "Tunable and switchable multiwavelength fiber lasers with broadband range based on nonlinear polarization rotation technique," *Opt. Eng.* **49**(9), 094303 (2010).
13. X. H. Li, Y. S. Wang, W. Zhao, W. Zhang, Z. Yang, X. H. Hu, H. S. Wang, X. L. Wang, Y. N. Zhang, Y. K. Gong, C. Li, and D. Y. Shen, "All-normal dispersion, figure-eight, tunable passively mode-locked fiber laser with an invisible and changeable intracavity bandpass filter," *Laser Phys.* **21**(5), 940–944 (2011).
14. Z. C. Luo, A. P. Luo, and W. C. Xu, "Tunable and switchable multiwavelength passively mode-locked fiber laser based on SESAM and inline birefringence comb filter," *IEEE Photon. J.* **3**(1), 64–70 (2011).
15. X. Wang, Y. Zhu, P. Zhou, X. Wang, H. Xiao, and L. Si, "Tunable, multiwavelength Tm-doped fiber laser based on polarization rotation and four-wave-mixing effect," *Opt. Express* **21**(22), 25977–25984 (2013).
16. X. Liu, X. Zhou, X. Tang, J. Ng, J. Hao, T. Y. Chai, E. Leong, and C. Lu, "Switchable and tunable multiwavelength erbium-doped fiber laser with fiber Bragg gratings and photonic crystal fiber," *IEEE Photon. Technol. Lett.* **17**(8), 1626–1628 (2005).
17. H. B. Sun, X. M. Liu, L. R. Wang, X. H. Li, and D. Mao, "Spacing-tunable multi-wavelength fiber laser based on cascaded four-wave mixing in highly nonlinear photonic-crystal fiber," *Laser Phys.* **20**(11), 1994–2000 (2010).
18. Z. Q. Luo, J. Z. Wang, M. Zhou, H. Y. Xu, Z. P. Cai, and C. C. Ye, "Multiwavelength mode-locked erbium-doped fiber laser based on the interaction of graphene and fiber-taper evanescent field," *Laser Phys. Lett.* **9**(3), 229–233 (2012).
19. M. Sun, J. Y. Long, X. H. Li, Y. Liu, H. F. Ma, Y. An, X. H. Hu, Y. S. Wang, C. Li, and D. Y. Shen, "Widely tunable Tm:LuYAG laser with a volume Bragg grating," *Laser Phys. Lett.* **9**(8), 553–556 (2012).
20. S. Zhao, P. Lu, D. Liu, and J. Zhang, "Switchable multiwavelength thulium-doped fiber ring lasers," *Opt. Eng.* **52**(8), 086105 (2013).
21. S. M. Kobtsev, S. V. Kukarin, and Y. S. Fedotov, "Wide-spectrally-tunable CW and femtosecond linear fiber lasers with ultrabroadband loop mirrors based on fiber circulators," *Laser Phys.* **20**(2), 347–350 (2010).
22. C. V. Shank, R. Yen, and C. Hirlimann, "Time-resolved reflectivity measurements of femtosecond-optical-pulse-induced phase transitions in silicon," *Phys. Rev. Lett.* **50**(6), 454–457 (1983).
23. D. Y. Tang, L. M. Zhao, B. Zhao, and A. Q. Liu, "Mechanism of multisoliton formation and soliton energy quantization in passively mode-locked fiber lasers," *Phys. Rev. A* **72**(4), 043816 (2005).
24. S. M. J. Kelly, "Characteristic sideband instability of periodically amplified average soliton," *Electron. Lett.* **28**(8), 806–808 (1992).
25. S. Kobtsev, S. Smirnov, S. Kukarin, and S. Turitsyn, "Mode-locked fiber lasers with significant variability of generation regimes," *Opt. Fiber Technol.* **20**(6), 615–620 (2014).
26. M. L. Dennis and I. N. Duling III, "Intracavity dispersion measurement in modelocked fibre laser," *Electron. Lett.* **29**(4), 409–411 (1993).
27. D. Y. Tang, J. Wu, L. M. Zhao, and L. J. Qian, "Dynamic sideband generation in soliton fiber lasers," *Opt. Commun.* **275**(1), 213–216 (2007).
28. L. M. Zhao, D. Y. Tang, X. Wu, H. Zhang, C. Lu, and H. Y. Tam, "Observation of dip-type sidebands in a soliton fiber laser," *Opt. Commun.* **283**(2), 340–343 (2010).

## 1. Introduction

Multiwavelength fiber laser can be widely used in wavelength division multiplexing communication, optical signal processing, optical sensing, and precision spectroscopy [1,2]. There are many methods to realize multiwavelength lasing. Zhang *et al.* obtained the dual- and tri- wavelength dissipative soliton by the artificial birefringence filter to affect the homogenous gain in an Er-doped fiber laser [3]. Zhao *et al.* realized the switchable dual-wavelength mode-locked state around 1550 nm by inserting a tunable attenuator in the cavity to change the intracavity loss [4]. Chamorovskiy *et al.* demonstrated the dual-wavelength soliton pulse in Ho-doped fiber laser by adjusting the polarization controller (PC) in the cavity [5]. Wang *et al.* used the cascaded filter structure to construct the 2  $\mu\text{m}$  switchable dual-wavelength continuous wave (CW) fiber laser [6]. Nonlinear polarization evolution (NPE) and nonlinear optical loop mirror are often used by many researchers to induce wavelength- or intensity-dependent loss of the cavity to alleviate the mode competition caused by the homogeneous gain broadening [7–13]. The hybrid mode-locked technique (semiconductor saturable absorber mirror and nonlinear polarization rotation) can also achieve multi-wavelength mode-locking operation [14]. Some specialty or long haul fibers can be incorporated into laser cavities to generate multi-wavelength lasing, for examples, a 400 meter single-mode fiber (SMF) [15] or photonic crystal fiber [16,17] was used to enhance the four-wave mixing effect and suppress the polarization mode competition; a polarization-maintaining fiber (PMF) together with the PCs was employed to act as the Lyot birefringence

filter [1]; a Graphene-deposited fiber-taper has been used as a spectral filter [18]; a volume Bragg grating can work as a tunable filter [19], and a multimode fiber has taken the role of a spatial mode beating filter [20].

There have been other methods using additional components in the laser cavity, such as optical filters, fiber gratings, or PMF to realize multiwavelength lasing, which however increase the complexity of the laser cavity. So far, the operating wavelengths of these multiwavelength fiber lasers have been mainly in the 1  $\mu\text{m}$  to 1.5  $\mu\text{m}$  regimes [3] [21]. Only few papers report the multiwavelength fiber laser in 2  $\mu\text{m}$  regime, and most of these 2  $\mu\text{m}$  lasers operate in the CW lasing mode. However, the main challenge of stable pulsed multiwavelength laser is the strong homogeneous line broadening of Tm-doped fiber, and many applications, e.g. time-resolved phenomena and measurements [22], require pulsed emission of a laser, especially tunable and switchable operation. While, tunable and switchable dual-wavelength pulsed lasing in 2  $\mu\text{m}$  regime has not been reported, to the best of our knowledge.

In this paper, tunable and switchable dual-wavelength mode locking is experimentally demonstrated in a Tm-doped fiber laser. The proposed fiber laser can realize tunable single-wavelength mode locking. The fiber laser is mode-locked by the NPE technique. The NPE also induces wavelength-dependent loss. It alters the effective gain (net gain minus cavity loss) broadening of Tm-doped fiber from homogeneous to inhomogeneous, and alleviates the mode competition at different wavelengths, thus making multiwavelength mode locking feasible. The wavelength tunability results from the NPE induced wavelength-dependent loss (tune the cavity transmission). Switchable operation with one soliton appears at each time is realized in a repeatable manner.

## 2. Experimental setup

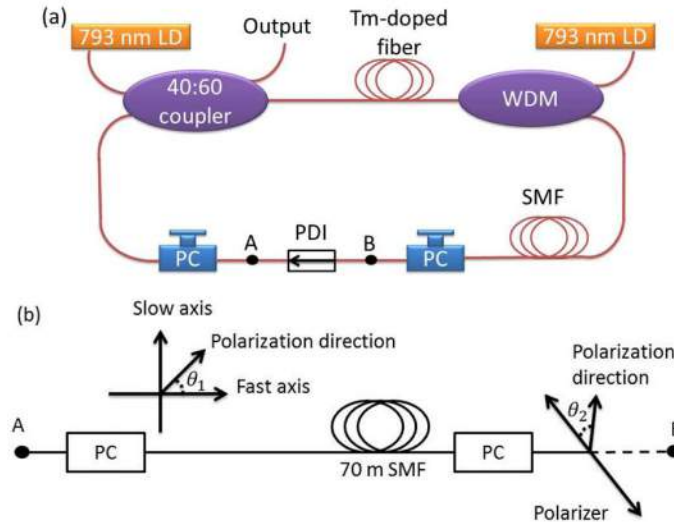


Fig. 1. (a) The setup and (b) the operating principle of tunable and switchable multiwavelength mode-locked Tm-doped fiber laser using nonlinear polarization evolution. LD: laser diode. WDM: wavelength-division multiplexer. PC: polarization controller. PDI: polarization-dependent isolator. SMF: Single-mode fiber.

Figure 1(a) is the experimental setup. A 1.5 m Tm-doped single mode fiber (Nufern, core/cladding diameter: 9/125  $\mu\text{m}$ ) is used as the gain medium for laser emission at the wavelength regime around 1860 nm. It is bidirectionally pumped by two 793 nm laser diodes (LD) with maximum output power of 170 and 200 mW, respectively. The pump light from one LD is coupled into the cavity by a wavelength-division multiplexer (WDM), and the

pump light from the other LD is launched into the cavity by a  $2 \times 2$  40:60 coupler, which also acts as the output coupler. For this coupler, 100% of 793 nm pump light will be coupled into the cavity except the insertion loss, ~40% of the 1860 nm light will circulate inside the cavity and 60% will be outputted. The active Tm-doped fiber has a group velocity dispersion of 35 ps/nm/km at 1860 nm. The group velocity dispersion of the 70 m silica SMF is 33 ps/nm/km at 1860 nm, which is used as the birefringent fiber. The total anomalous dispersion supports the soliton propagation in the laser cavity. With 1 m fiber pigtail in the coupler, WDM and polarization-dependent isolator (PDI), the total cavity length is around 77.5 m. Mode locking of the fiber laser is achieved by NPE formed by two PCs and a PDI. Since the PDI contains two polarizers, the output light from the isolator (point A in Fig. 1(b)) will be linear-polarized. Then the polarization of the light will be changed by PC1,  $\theta_1$  is the angle between the polarization direction of the light and the fast axis of the birefringent fiber. The light propagates through the birefringent fiber and PC2, and reaches the other polarizer inside the PDI with an angle of  $\theta_2$ , which is the angle between the orientation of polarizers and the fast axis of the birefringent fiber. The polarizers inside PDI, the PCs and the birefringent fiber can change the cavity loss. The transmission function of the setup can be described as [23]:

$$T = \cos^2 \theta_1 \cos^2 \theta_2 + \sin^2 \theta_1 \sin^2 \theta_2 + \frac{1}{2} \sin(2\theta_1) \sin(2\theta_2) \cos(\Delta\varphi_L + \Delta\varphi_{NL}) \quad (1)$$

$\Delta\varphi_L$  and  $\Delta\varphi_{NL}$  are the linear and nonlinear cavity phase delay, which can be expressed as, respectively,

$$\Delta\varphi_L = 2\pi L(n_x - n_y) / \lambda \quad (2)$$

$$\Delta\varphi_{NL} = 2\pi n_2 PL \cos(2\theta_1) / \lambda A_{eff} \quad (3)$$

Where  $L$  is the length of birefringent fiber,  $|n_x - n_y| = B_m$  is the strength of modal birefringence,  $P$  is the instantaneous power of input signal,  $n_2$  is the nonlinear refractive index,  $\lambda$  is the operating wavelength, and  $A_{eff}$  is the effective mode area. By rotating or squeezing the PCs, the  $\theta_1$ ,  $\theta_2$  and  $B_m$  will change so that the cavity transmission  $T$  will change. This will change the effective broadening of Tm-doped fiber from homogeneous into inhomogeneous. Thus, the multiwavelength mode-locked lasing can be achieved.

The output is connected to an optical spectrum analyzer and a 33 GHz oscilloscope together with a 7 GHz photodetector to simultaneously measure the spectra and the pulse train using a 50/50 coupler.

### 3. Experimental results

#### 3.1. Tunable single-wavelength mode locking

By increasing the pump power to 300 mW, the single- and dual-wavelength CW lasing operation can be easily obtained by changing the PCs. The dual-wavelength CW lasing can be switchable. By further changing the PCs, the stable single-wavelength mode locking appears with the center wavelength of 1862 nm and the 3-dB bandwidth is 3.5 nm (Fig. 2(a)). The spectrum exhibits Kelly sidebands, which is the typical feature of soliton in anomalous-dispersion fiber lasers [24]. The full width at half maximum (FWHM) of the pulse is 3.1 ps measured at 1862 nm (Fig. 2(b)). The time-bandwidth-product is 0.944, indicating that the intra-cavity pulses are chirped. The mode-locked pulses can be compressed through dechirping outside the laser cavity with dispersion compensating fibers or grating pairs. The repetition rate is 2.68 MHz as illustrated in Fig. 2(c) which exactly corresponds to the cavity round-trip frequency. The output power is 3 mW due to the loss of long SMF and the 40:60 coupler.

When increasing the pump power to 350 mW, the lasing wavelength can be tuned with a wavelength range of 34 nm from 1852 ~1886 nm by either rotating or squeezing the PCs (Fig. 2(d)).

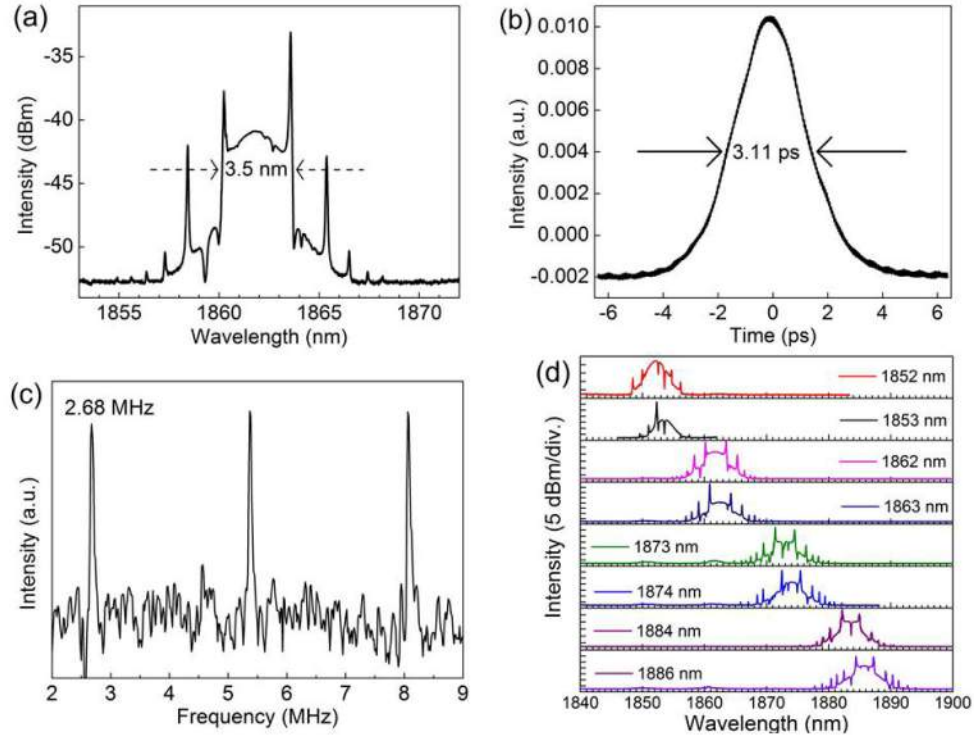


Fig. 2. (a) Spectrum, (b) pulse width and (c) RF spectrum of mode-locked single-wavelength laser at 1862 nm. (d) Tunable single-wavelength mode locking with tuning range from 1852 nm to 1886 nm.

### 3.2. Tunable and switchable dual-wavelength mode locking

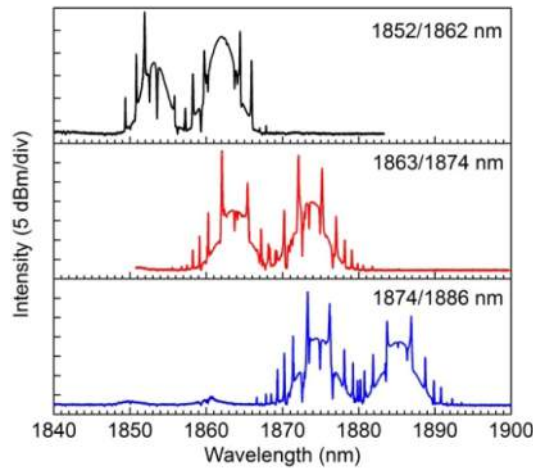


Fig. 3. Tunable dual-wavelength mode locking with the center wavelength of 1852/1862 nm, 1863/1874 nm, and 1874/1886 nm. A wide tuning range from 1852 nm to 1886 nm can be achieved.

By further tuning the PCs without changing the pump power, dual-wavelength mode locking appears. The separation between the two wavelengths is around 10 nm. By slightly rotating or squeezing the PCs, dual-wavelength mode locking can be tuned from 1852 to 1886 nm (Fig. 3), with the center wavelength of 1852/1862 nm, 1863/1874 nm, and 1874/1886 nm. The separation between the two wavelengths remains around 10 nm, and the two lasing wavelengths simultaneously shift about 10 nm. At 1852/1862 nm, 1863/1874 nm and 1874/1886 nm, the dual-wavelength lasing is switchable, one of them with the center wavelength of 1852/1862 nm is illustrated in Fig. 4(a). The oscilloscope trace shows that there are two soliton pulses propagating in the cavity (Fig. 4(b)). The two solitons correspond to the two wavelengths since we use one 50/50 coupler to measure the pulse train and spectrum simultaneously. In dual-wavelength mode-locked operation, the spectrum shows two peaks, which are the center wavelengths of the two solitons respectively. Under this condition, the pulse train on the oscilloscope is observed to be highly stable. It is the difference in the group velocities of the two solitons makes them located in different positions in the time domain.

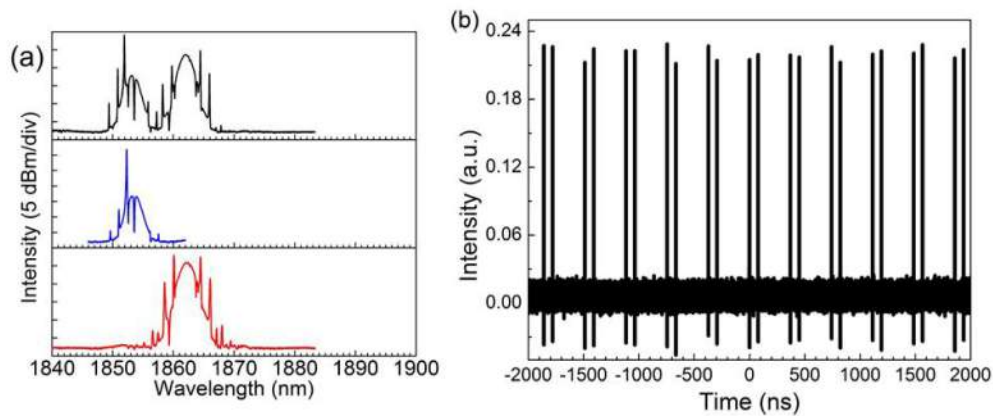


Fig. 4. (a) Switchable dual-wavelength mode locking at 1852 and 1862nm. (b) Pulse train of dual-wavelength mode locking.

#### 4. Discussion

In this setup, the mode locking has many regimes, including multi-soliton state, single-scale state, wave-packet state, tunable single-wavelength state, tunable and switchable dual-wavelength state [23,25]. If other researchers implement a similar laser, they may observe the regimes listed above. In this paper, we only focus on the tunable single-wavelength, tunable and switchable dual-wavelength mode locking.

The tunable and switchable dual-wavelength mode locking can be repeatable in the experiment. But the center wavelength maybe shifts a little from the values shown in this paper, which is due to the NPE effect. The tunable and switchable capability of our setup is achieved in the single-scale regime through two steps. The first step is coarse adjustment of the PCs to get the stable single-scale pulses. The second step is fine adjustment of the PCs around that position to get the tunable and switchable mode locking.

The above spectra show that two types of sideband are generated. One is the peak-type sidebands. It is formed by the constructive interference between the soliton and dispersive waves [24]. The position offset of the peak from the center wavelength is determined by the cavity dispersion and length [26]. Solitons operating at different wavelengths have different dispersions, thus the peak offsets from the center wavelength are different among these solitons (Fig. 3). The other is the dip-type sidebands. It is a new resonance between the soliton and the dispersive wave when the soliton intensity varies. The variation is due to the cavity

output coupling, lossy fiber intervals, and laser gain amplification. In the resonance, the energy flows either from soliton to dispersive waves or from dispersive waves to soliton, depending on the phase of soliton and dispersive waves [27,28]. If the energy is from soliton to dispersive waves, a dip on the spectrum appears. When tuning the PCs, the phase of soliton and dispersive waves will be changed. Consequently, the dip-sidebands appear.

The formation of dual-wavelength laser can be explained as follows. The laser emission spectrum is a Lorentz-shaped curve depending on the wavelength, according to the data from fiber manufacturer. If the cavity transmission is independent of wavelength, the laser emits at the point where total cavity effective gain is the maximum, which is single-wavelength laser emission. In order to have the multiwavelength laser emission, the cavity transmission should be a periodic function to achieve multiple maximum points for the total cavity effective. The period of transmission function equals to the wavelength separation between the two peaks in the dual-wavelength emission. The period of cavity transmission is related to  $\cos(\Delta\varphi_L + \Delta\varphi_{NL})$  from Eq. (1), and the separation of wavelength  $\Delta\lambda = \lambda_1 - \lambda_2$  in one period satisfy:

$$\Delta(\Delta\varphi_L + \Delta\varphi_{NL}) = (\Delta\varphi_{L1} + \Delta\varphi_{NL1}) - (\Delta\varphi_{L2} + \Delta\varphi_{NL2}) = 2\pi \quad (4)$$

$$\left[ L(n_x - n_y) + n_2 PL \cos(2\theta_1) / A_{eff} \right] \left( \frac{1}{\lambda_1} - \frac{1}{\lambda_2} \right) = 1 \quad (5)$$

We substitute the frequency  $f$  for  $\lambda$ ,

$$\Delta f = \frac{c}{L(n_x - n_y) + n_2 PL \cos(2\theta_1) / A_{eff}} \quad (6)$$

In this setup,  $L = 70 \text{ m}$ ,  $P = 0.003 \text{ W}$ ,  $n_2 = 2.7 \times 10^{-20} \text{ m}^2 / \text{W}$ , mode-field diameter is  $12.4 \mu\text{m}$ . By choosing  $\theta_1 = 3\pi/4$ ,  $B_m = 4.9 \times 10^{-6}$ , the  $\Delta\lambda$  is around 10 nm, which agrees well with the experimental results. The corresponding transmission spectra with different value of  $\theta_2$  are shown in Fig. 5(a). The comparison between simulation and experimental results is shown in Fig. 5(b).

From Fig. 5(a), there should be simultaneously multiple-wavelength soliton emission theoretically, however we can only see dual-wavelength soliton emission. It is due to the competition between each soliton, which reduces the possibility of multiple solitons emission at the same time. The modulation depth of cavity transmission is different when  $\theta_1$  or  $\theta_2$  is changed. The competition between each soliton will be different. Thus at each changing of  $\theta_1$  or  $\theta_2$  by tuning the PCs, the dual-wavelength soliton at center wavelength of 1852/1862 nm, 1863/1874 nm, and 1874/1886 nm are observed.



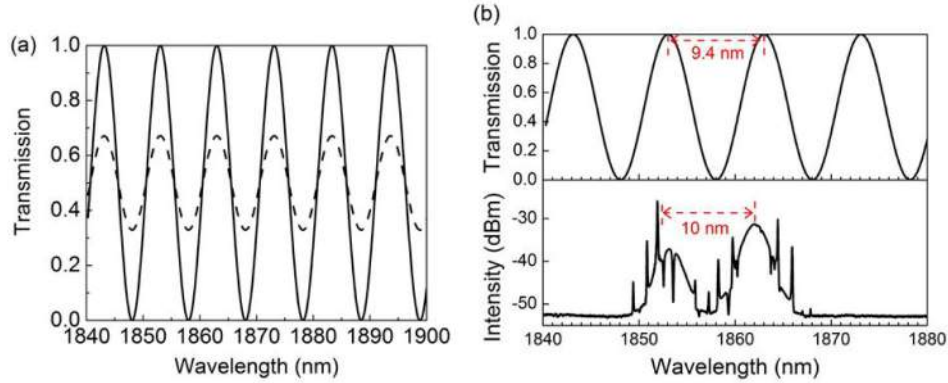


Fig. 5. (a) The simulation transmission spectrum with the wavelength from 1840 to 1900 nm. The solid curve  $\theta_2 = \pi/4$ , the dash curve  $\theta_2 = \pi/18$ . (b) The comparison between simulation and experimental results.

## 5. Conclusion

We have demonstrated both tunable and switchable dual-wavelength mode locking in an ultrafast Tm-doped fiber laser by the NPE technique. The tunable and switchable operation results from the wavelength-dependent loss of the cavity induced by the NPE effect. For the dual-wavelength operation, three pairs of dual-soliton with center wavelengths of 1852/1862 nm, 1863/1874 nm, and 1874/1886 nm can be observed. Switchable operation with one soliton appear at each time is realized. All the switchable or tunable operation is realized by simply rotating or squeezing the PCs. This provides a simple and compact solution to multiwavelength and tunable mode locking in fiber lasers. This fiber laser will find spreading applications in optical signal processing, sensing, material engineering, and optical communications.

## Acknowledgments

The authors thank Dr. Biao SUN, and Ms. Yanyan ZHOU for useful discussions, Prof. Dingyuan TANG, Mr. Guodong SHAO and Dr. Lam Quoc Huy for equipment support. We would like to acknowledge financial support from A\*STAR SERC Innovation in Remanufacturing Programme (Grant No. 112 290 4018) and A\*STAR SERC Advanced Optics in Engineering Programme (Grant No. 122 360 0004).